A FULL-WAVE ANALYSIS OF SHIELDED MICROSTRIP LINE-TO-LINE TRANSITIONS †

T.S. Horng, H.Y. Yang, and N.G. Alexopoulos

Electrical Enginering Department, University of California, Los Angeles
Los Angeles, CA 90024

Abstract

A rigorous procedure is used to analyze several microstrip line-to-line transitions in a shielded multi-layer structure. The transitions studied include edge-coupled lines, overlay-coupled lines and coupled-to-single lines. A power conservation check based on a rigorous Poynting vector analysis is also used to determine the accuracy of the numerical convergence. The results of power distributions and coupling coefficients of the line-to-line transitions are studied parametrically to indentify the properties and applications of each transition.

Introduction

Proximity-coupled line-to-line transitions are important building blocks for high frequency interconnects. Applications in millimeter-wave integrated circuits include high-pass filters, multiplexers and directional couplers. Losch [1] has designed a broadband highpass filter in realization of an overlay coupled line transition based on a quasi-static formulation. A more rigorous full wave analysis for coupled line filters associated with the open structure has been discussed by Katehi [2] for an edge-coupled transition and by Yang and Alexopoulos [3] for an overlay-coupled transition. In [3] a spectral-domain approach by expanding the current in the coupled line section with a combination of entire domain and subdomain modes is used. This mode expansion machanism seems to be the most efficient and fruitful by far. For the advantage of preventing unnecessary interaction and radiation loss, a waveguide housing is sometimes more common and practical in the real circuit design. In this work, a full-wave moment method is used to characterize shielded microstrip line-to-line transitions.

Method of Moments

Several different types of electromagnetically coupled lines as shown in Figs. 1-3 are investigated. The methodology applied here is in analogy to that reported in [3], however, the spectral Green's function and the numerical procedure are very much different. Since the line-offset and the width of microstrips in shielded structures are comparable to the waveguide dimensions, the transverse current component should not be neglected and complete dyadic Green's function of a multi-layer waveguide is required. The integral equation after a Galerkin's procedure can be converted into a set of linear equations, when expressed in matrix form:

$$\begin{bmatrix} [Z_{11ss}] & [Z^{ref}_{11se}] & [Z_{12ss}] & [Z^{tra}_{12se}] \\ [Z_{21ss}] & [Z^{ref}_{21se}] & [Z_{22ss}] & [Z^{tra}_{22se}] \end{bmatrix} \begin{bmatrix} [I_{1s}] \\ -\Gamma \\ [I_{2s}] \\ T \end{bmatrix} = \begin{bmatrix} [I^{inc}_{11se}] \\ [I^{inc}_{21se}] \end{bmatrix} \tag{1}$$

where each submatrix [Z], due to the presence of both x and z directed currents, contains 4 submatrices, for example:

$$[Z_{11ss}] = \begin{bmatrix} [Z_{11sszz}] & [Z_{11sszx}] \\ [Z_{12sszz}] & [Z_{11sszx}] \end{bmatrix} \tag{2}$$

and submatrix [I] and [I^{inc}] contain two submatrices as follows:

† This research was performed under U.S. Army Research Office Grant DAAL 03-86-k-0090

$$[I_{1s}] = \begin{bmatrix} [I_{1z}] \\ [I_{1x}] \end{bmatrix} \quad (3)$$

$$\left[I^{inc}_{11se}\right] = \begin{bmatrix} [I^{inc}_{11ze}] \\ [I^{inc}_{11xe}] \end{bmatrix} \quad (4)$$

Each element in these submatrices represents the reaction of different basis functions. For instance, the elements of $[Z_{12ssxz}]$ are the reaction between x-directed currents of subdomain mode associated with microstrip 1 and z-directed currents of subdomain mode associated with microstrip 2. These subdomain modes are basically either PWS functions or pulse functions. The entire domain modes are composed of the reflected mode, transmitted mode, and incident mode which are distinguished with abbreviation *ref*, *tra*, and *inc*, respectively. The computation of each element requires both infinite summation and integration in spectral domain and their expressions are in the general form of:

$$Z^{kl}_{ijss\hat{u}_1\hat{u}_2} = \sum_{n=-\infty}^{\infty} \int_{-\infty}^{\infty} \tilde{G}_{ij\hat{u}_1\hat{u}_2}(\alpha_n, \beta) \tilde{J}_{it\hat{u}_1}(\alpha_n) \tilde{J}_{jt\hat{u}_2}(\alpha_n) \tilde{f}^k_{i\hat{u}_1}(\beta) \tilde{f}^l_{j\hat{u}_2}(\beta)^* d\beta \quad (5)$$

and

$$Z^{k\ p}_{ijse\hat{u}_1\hat{u}_2} = \sum_{n=-\infty}^{\infty} \int_{-\infty}^{\infty} \tilde{G}_{ij\hat{u}_1\hat{u}_2}(\alpha_n, \beta) \tilde{J}_{it\hat{u}_1}(\alpha_n) \tilde{J}_{jt\hat{u}_2}(\alpha_n) \tilde{f}^k_{i\hat{u}_1}(\beta) \tilde{J}^{e\ p}_{jl\hat{u}_2}(\beta)^* d\beta \quad (6)$$

where $\tilde{G}_{ij\hat{u}_1\hat{u}_2}$ is the spectral-domain dyadic Green's function. Superscript p identifies different entire domain modes. $\tilde{J}_{it\hat{u}}$ is the Fourier transform of transverse dependence and $\tilde{f}^k_{i\hat{u}}, \tilde{J}_{il\hat{u}}$ are Fourier transform of longitudinal dependence with respect to subdomain and entire domain modes, respectively.

Power Conservation Check

For shielded microstrip transitions, the convergence of the moment method solution is very sensitive to the type and number of expansion functions chosen. Power conservation provides a nice way of checking the accuracy of the solution. According to the configurations shown in Figs. 1-3, the incident power should be equal to the summation of reflected power, transmitted power and some loss coupled to the multi-layered waveguide modes. With proper waveguide dimension, the loss coupled to the waveguide modes can be removed and the expression of power conservation can be simply written as

$$|\Gamma|^2 + \frac{Z_{c2}}{Z_{c1}} |T|^2 = 1 \quad (7)$$

where Z_{c1} and Z_{c2} are the characteristic impedance of feed line and parasitic coupled line respectively. A frequency-dependent method of computing the characteristic impedance of both single and coupled microstrip transmission lines described in [4, 5] can be used to determine the accuracy of the numerical results given in this work. In the present computations of the transition problems, entire domain modes of 3 guided wavelength and 9 to 18 subdomain modes are used in each microstrip line. The convergence has been checked within 1% accuracy. The power conservation is also checked with good consistency. An example of this check is shown in Table I.

Numerical Results and Discussions

From Figs. 5 – 11, the maximum coupling occurs around $ovl = \frac{1}{4}\lambda_{go}$ (λ_{go} is the wavelength of the odd-mode guided in the coupled line section) with a wide frequency-insensitive range. This implies that the transitions are broad-band and are very useful in many MMIC applications. Besides, from Figs. 5 – 8, the coupling efficiency is better in overlay line-to-line transition than in edge coupled line-to-line transition. This indicates the former will be a promising element in realization of millimeter wave high-pass filter.

Figs. 9 — 10 show the results for the case of an overlay coupled-to-single microstrip transition. It is seen that the even-mode coupling depends less on the line-offset of parasitic coupled line, as compared with single-line coupling. It is also noted that the even-mode of coupled lines can couple energy to a centered parasitic microstrip line while the odd-mode can not. This may find applications in a phase detector.

The frequency response of an overlay-coupled microstrip transition is shown in Figs. 11 — 12. The geometrical parameters are specially designed in the coupled section where the line-width is much larger than the spacing between two lines. It is seen that, in a wide frequency range, the coupling coefficient is almost independent of frequency. In addition, it is possible to couple more than 95% of the total power through the discontinuity. This geometry (so called

ovl	$\lvert\Gamma\rvert^2+\frac{z_{c2}}{z_{c1}}\lvert T\rvert^2$	ovl	$\lvert\Gamma\rvert^2+\frac{z_{c2}}{z_{c1}}\lvert T\rvert^2$
- 0.05	1.000	0.13	0.997
- 0.03	1.000	0.15	0.999
- 0.01	1.001	0.17	1.004
0.01	1.003	0.19	1.003
0.03	1.004	0.21	1.002
0.05	1.003	0.23	1.001
0.07	1.001	0.25	1.000
0.09	1.001	0.27	1.000
0.11	0.999	0.29	0.999

Table 1. Power conservation check for the configuration of Fig. 2. Both $|\Gamma|$ and $|T|$ are the same as those in Figs. 7 and 8.

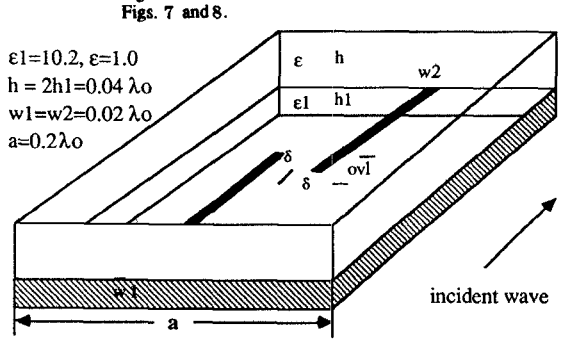

Fig. 1 Edge coupled line-to-line transition

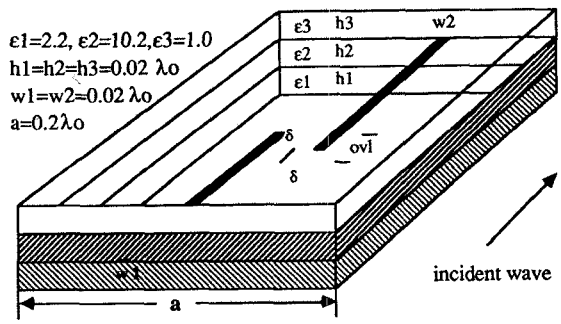

Fig. 2 Overlay coupled line-to-line transition

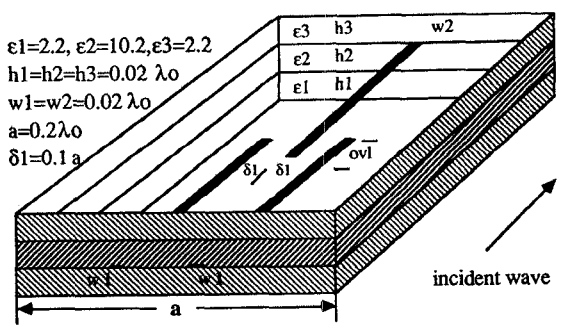

Fig. 3 Overlay coupled-to-single line transition

suspended stripline) may be very useful due to these two excellent characteristics.

Conclusions

In this work, a full-wave analysis is proposed to develop a generalized dynamic model for several types of shielded microstrip line-to-line transitions. The results obtained from the method of moments are checked within 1% accuracy by power conservation. The results presented also show excellent properties in some transitions and may find promising applications in MMIC coupler and filter design.

References

[1] L.E. Losch, "Design Procedure for inhomogeneous coupled line sections," IEEE Trans. on Microwave Theory and Techniques, Vol. MTT-36, pp. 1186-1190, July 1988.

[2] P.B. Katehi, "Radiation losses in MM-wave open microstrip filters," Electromagnetics, vol.7, pp. 137-152, 1987.

[3] H.Y. Yang and N.G. Alexopoulos, "Basic building blocks for high frequency interconnects: theory and experiment,: IEEE Trans. on Microwave Theory and Techniques, Vol. MTT-36, pp.1258-1264, Aug. 1988.

[4] M.K. Krage and G.I. Haddad, "Frequency-dependent characteristics of microstrip transmission lines," IEEE Trans. on Microwave Theory and Techniques, Vol. MTT-20, pp. 678-686, Oct. 1972.

[5] A. Nakatani and N.G. Alexopoulos, "Toward a generalized algorithm for the modeling of dispersive properties of integrated circuit structures on anisotropic substrates," IEEE Trans. on Microwave Theory and Techniques, Vol. MTT-33, pp. 1436-1441, Dec. 1985.

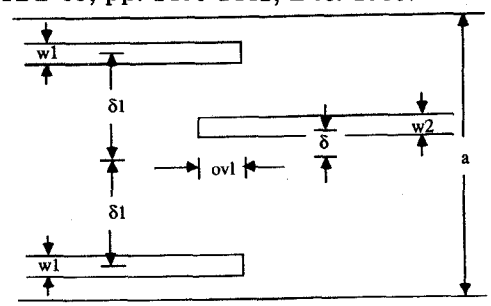

Fig. 4 Top view for Fig. 3

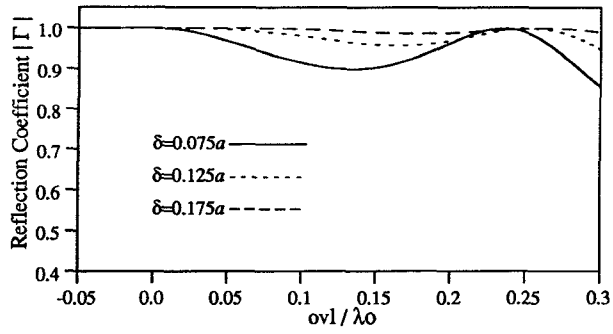

Fig. 5 $|\Gamma|$ versus overlap for the configuration of Fig. 2.1

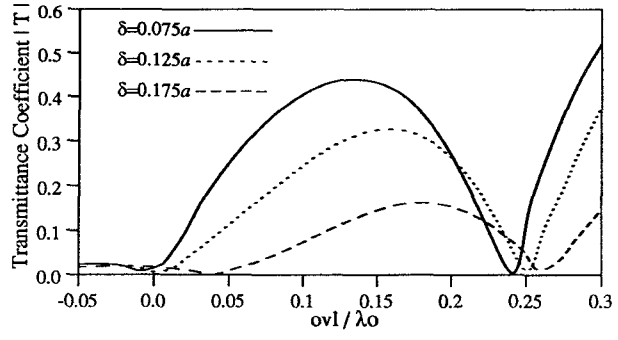

Fig. 6 $|T|$ versus overlap for the configuration of Fig. 2.1

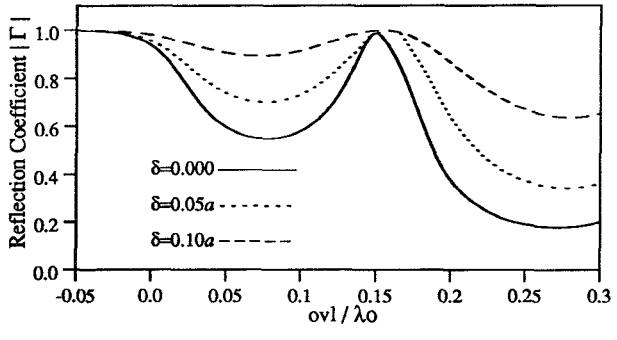

Fig. 7 $|\Gamma|$ versus overlap for the configuration of Fig. 2.2

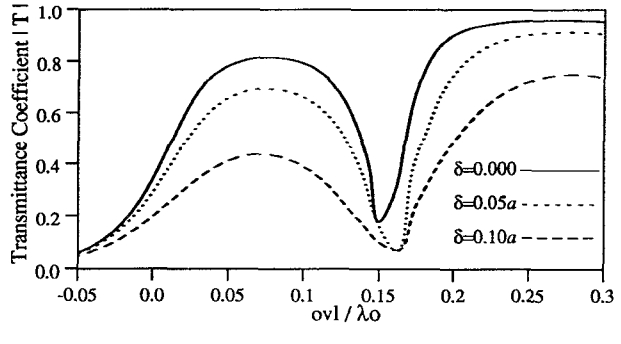

Fig. 8 $|T|$ versus overlap for the configuration of Fig. 2.2

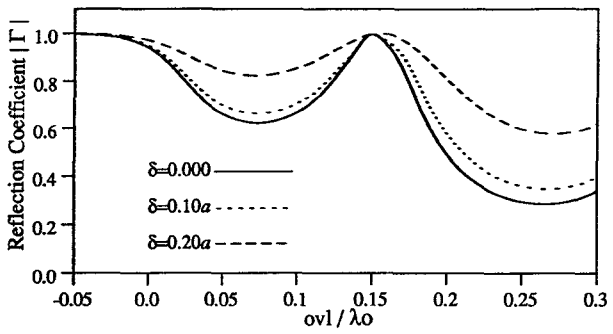

Fig. 9 $|\Gamma|$ versus overlap for even-mode excitation. (configuration Fig. 2.3)

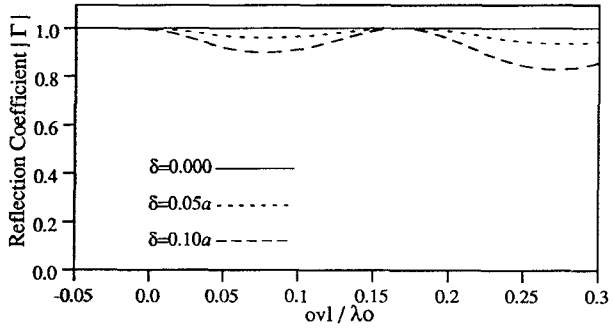

Fig. 10 $|\Gamma|$ versus overlap for odd-mode excitation. (configuration Fig. 2.3)

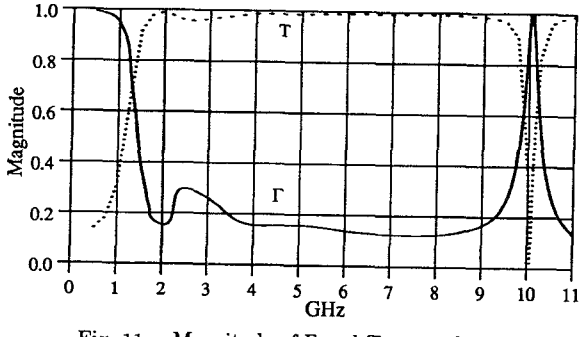

Fig. 11 Magnitude of Γ and T versus frequency.

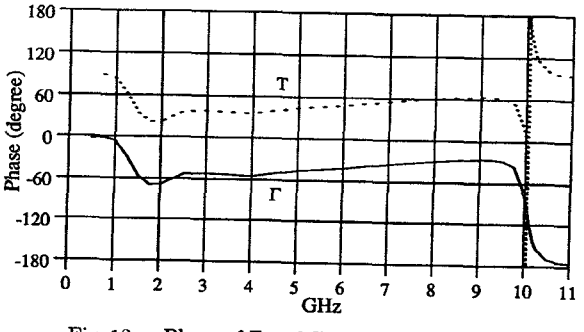

Fig. 12 Phase of Γ and T versus frequency. Geometrical parameters: $\epsilon_1 = \epsilon_3 = 1, \epsilon_2 = 10.2$, $h_1 = h_3 = 70mil, h_2 = 10mil, w_1 = w_2 = 50mil$, $\delta_1 = \delta_2 = 0, ovl = 185mil, a = 500mil$